

Magnetic properties and crystal structure of the dichlorobis(1-allyltetrazole)cobalt(II) complex

Yu. G. Shvedenkov,* A. V. Virovets, and L. G. Lavrenova

A. V. Nikolaev Institute of Inorganic Chemistry, Siberian Branch of the Russian Academy of Sciences,
3 ul. Lavrent'eva, 630090 Novosibirsk, Russian Federation.
Fax: +7 (383 2) 34 4489. E-mail: schved@tomo.nsc.ru

The cobalt(II) chloro complex with 1-allyltetrazole (Alltz) $\text{Co}(\text{Alltz})_2\text{Cl}_2$ was studied by the magnetic susceptibility measurements and X-ray diffraction analysis. The coordination polyhedron of the complex is a distorted octahedron formed by the N(4) atoms of two Alltz cycles and four bridging Cl atoms (coordination unit CoN_2Cl_4). Each chlorine atom is bound with two cobalt atoms giving rise to a crimped polymeric network. The $\text{Co}(\text{Alltz})_2\text{Cl}_2$ complex is a weak ferromagnetic with $T_N = 102 \pm 1$ K and spontaneous magnetization $\sigma_S(5 \text{ K}) = 710 \pm 5 \text{ G cm}^3 \text{ mol}^{-1}$. Hysteresis effects, depending on the intensity of the magnetic field in which the sample was cooled, were detected.

Key words: molecular magnet, cobalt, tetrazole, complex, X-ray diffraction analysis, magnetochemistry, weak ferromagnetic.

A search for new metal complexes characterized by transitions to the magnetically ordered state or spin transitions is a challenge of coordination chemistry. Tetrazoles, in particular, 1-substituted derivatives, represent a promising class of ligands for the synthesis of complexes possessing these properties.

The synthesis and study of the Co^{II} , Ni^{II} , and Cu^{II} compounds with 1-vinyl- (Vtz) and 1-allyltetrazoles (Alltz) have been reported.^{1–3} The $\text{Cu}(\text{Vtz})_2\text{Cl}_2$ and $\text{Cu}(\text{Alltz})_2\text{Cl}_2$ compounds demonstrated^{1,2} ferromagnetic ordering at the Curie temperatures of 11.5 and 10 K, respectively. According to the X-ray diffraction data, the structure of $\text{Cu}(\text{Alltz})_2\text{Cl}_2$ is layered-polymeric: the Cu^{II} coordination polyhedron is a square bipyramid in which the equatorial positions are occupied by two N(4) atoms of the Alltz cycle and two Cl atoms and the axial positions are occupied by two Cl atoms of the adjacent molecules of the complex.⁴ A similar structure is inherent⁵ in the Cu^{II} complex with 1-ethyltetrazole (Ettz) $\text{Cu}(\text{Ettz})_2\text{Cl}_2$.

In this work, we studied the structure and magnetic properties of the $\text{Co}(\text{Alltz})_2\text{Cl}_2$ complex (**1**) with 1-substituted tetrazole with the analogous layered-polymeric structure.

Experimental

Compound **1** was synthesized according to a previously described procedure.³ Well formed crystals of **1** as octagonal plates were grown from an EtOH solution by slow evaporation of the solvent at $\sim 20^\circ\text{C}$ for several days. The single crystal has the centrosymmetrical habitus: faces $\pm(100)$, distances between the faces 0.018 mm; $\pm(111)$, 0.40 mm; $\pm(1\bar{1}1)$, 0.43 mm;

$\pm(101)$, 0.21 mm; $\pm(110)$, 0.51 mm. Crystallographic data: monoclinic system, $a = 14.698(5) \text{ \AA}$, $b = 6.622(1) \text{ \AA}$, $c = 7.000(2) \text{ \AA}$, $\beta = 103.79(2)^\circ$, $V = 661.7(3) \text{ \AA}^3$, space group $P2_1/c$, $Z = 2$, $\rho_{\text{calc}} = 1.757 \text{ g cm}^{-3}$, $\mu = 13.901 \text{ mm}^{-1}$. The diffraction data were collected at $\sim 20^\circ\text{C}$ on a Syntex P2₁ four-circle automated diffractometer with a graphite monochromator using Cu-K α radiation ($\lambda = 1.5418 \text{ \AA}$). Intensities of 931 reflections were measured to $2\theta_{\text{max}} = 114^\circ$, and of them 892 reflections were independent ($R_{\text{int}} = 0.0537$). Corrections for absorption were applied by integration over the crystal perimeter using the SHELX-76 program, $T_{\text{min}}/T_{\text{max}} = 0.01951\text{--}0.56856$. The structure was solved by a combination of the Patterson and direct methods and refined using the least-squares method in the anisotropic (for non-hydrogen atoms) approximation using the SHELX-97 program package. All hydrogen atoms were localized from the difference synthesis of the electron density and refined in the isotropic approximation. Disordering of the allyl substituent was found by two positions with the weight 0.49(3)/0.51(3), which differ by the rotation about the N(1)–C(2) bond. The final divergence factors: $R_1 = 0.0361$, $wR_2 = 0.0912$ for 754 $F_{\text{hkl}} \geq 4\sigma(F)$; $R_1 = 0.0452$, $wR_2 = 0.0954$, and GOOF = 1.086 for all independent reflections using in calculations. The main bond lengths and bond angles are presented in Table 1. The coordinates of atoms were deposited with the Cambridge Structural Data Bank.⁶

The magnetic properties were studied with an SQUID magnetometer (Quantum Design) at 2–300 K with the external magnetic field intensity up to 30 kOe. Large (up to 4 mm) crystals of substance **1** were used in measurements. They were prepared along with single crystals for X-ray diffraction analysis and powdered before loading of the sample into a measuring ampule to avoid possible orientation effects. The weight of specimen **1** was 5.79 mg. Diamagnetism of atoms were taken into account by the additive Pascal scheme in calculations of the molar magnetic susceptibility (χ). The effective magnetic

Table 1. Main bond lengths (*d*) and bond angles (ω) in the structure of compound **1**

Bond	<i>d</i> /Å	Angle	ω /deg
Co—Cl(1)	2.539(1)	Cl(1) ^{#1} —Co—Cl(1) ^{#2}	180.0
Co—Cl(1) ^{#1}	2.538(1)	Cl(1) ^{#1} —Co—Cl(1)	87.16(2)
Co—N(4)	2.086(3)	Cl(1) ^{#2} —Co—Cl(1)	92.84(2)
N(1)—N(2)	1.342(5)	N(4)—Co—Cl(1) ^{#1}	90.8(1)
N(1)—C(1)	1.329(5)	N(4)—Co—Cl(1) ^{#2}	89.3(1)
N(1)—C(2)	1.457(7)	N(4)—Co—Cl(1)	90.73(10)
N(2)—N(3)	1.283(5)	N(4)—Co—Cl(1) ^{#3}	89.3(1)
N(3)—N(4)	1.362(5)	N(4) ^{#3} —Co—N(4)	180.0
N(4)—C(1)	1.307(6)	Co ^{#4} —Cl(1)—Co	143.24(4)
C(2)—C(3A)	1.39(1)	N(2)—N(1)—C(2)	123.6(4)
C(2)—C(3B)*	1.41(1)	C(1)—N(1)—N(2)	107.9(4)
C(4)—C(3A)	1.31(1)	C(1)—N(1)—C(2)	128.5(4)
C(4)—C(3B)*	1.29(1)	N(3)—N(2)—N(1)	107.5(3)
		N(2)—N(3)—N(4)	109.5(3)
		N(3)—N(4)—Co	127.7(3)
		C(1)—N(4)—Co	125.9(3)
		C(1)—N(4)—N(3)	106.5(3)

Note. The coordinates of atoms were transformed by the following symmetry procedures: ^{#1} *x*, $-y - 1/2$, $z - 1/2$; ^{#2} $-x$, $y + 1/2$, $-z + 3/2$; ^{#3} $-x$, $-y$, $-z + 1$; ^{#4} $-x$, $y - 1/2$, $-z + 3/2$.

* The second position of the disordered allyl substituent.

moment was determined in the paramagnetic region: $\mu_{\text{eff}} = [(3k/N_A\beta^2)\chi T]^{1/2} \approx (8\chi T)^{1/2}$, where *k* is the Boltzmann constant, *N_A* is Avogadro's number, and β is Bohr's magneton. The temperature of the magnetic phase transition was determined as an extremum of the derivative of the magnetic susceptibility with respect to temperature $\partial\chi/\partial T$.

Results and Discussions

The structure of complex **1** is layered-polymeric. The structure of the coordination unit is shown in Fig. 1. The structure of the compound is similar to that found^{4,5} for Cu(Alltz)₂Cl₂ and Cu(Ettz)₂Cl₂ by X-ray diffraction analysis. The coordination of the tetrazole ligand by the N(4) atom of the ring is monodentate. The coordination environment of the metal atom is the distorted octahedron 2 N + 4 Cl, where each Cl atom is bound to two Co atoms to form the crimped network (Fig. 2).

The main difference of the structure of complex **1** from those of Cu(Alltz)₂Cl₂ and Cu(Ettz)₂Cl₂ is that the Cu—μ-Cl bonds in the latters differ strongly in length (two distances are 2.30 Å each and two bonds are 2.99 Å each) due to the Jahn–Teller effect, while in Co(Alltz)₂Cl₂ the bridges are quite symmetrical (four bridges 2.54 Å each). The M—Cl—M angles do not virtually differ: 140–141° (copper complexes) and 143° (**1**). As in the copper compounds, in the structure of **1** the {MCl_{4/2}}_∞ layer is crimped in such a way that the Cl atoms are alternately shifted by 0.80 Å to the opposite sides from the plane formed by the Co atoms.

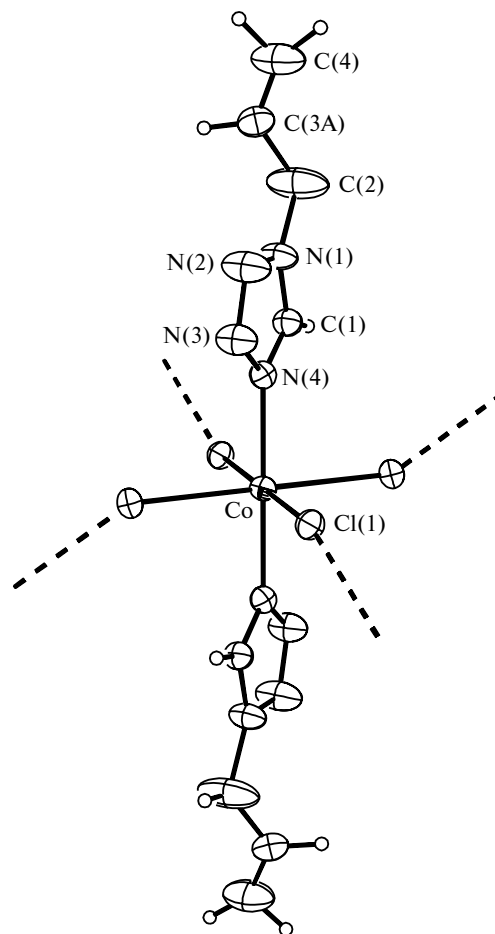


Fig. 1. Structure of the coordination unit of complex **1** (ellipsoids of atomic displacements of 50% probability). Only one position of the disordered allyl substituent is shown. The Co—Cl bonds forming the polymeric layer are shown by dotted lines.

The layered-polymeric structure found for crystal **1** was not observed previously for haloid compounds of cobalt(II). The published crystal structures of compounds with the octahedral environment of cobalt(II) atoms can conventionally be grouped as follows: (a) mononuclear complexes with terminal Cl atoms; (b) complexes containing two chloride bridges between Co atoms, including chain polymers with the {Co(L)(μ-Cl)₂Co(L)(μ-Cl)₂} structural motif, where L is the monodentate ligand; and (c) complexes with three chloride bridges between the Co atoms. The compounds in which metal atoms are bound by only one chloride bridge were previously synthesized for the Cu^{II} complexes instead of Co^{II}.

Analysis of the data on the Co—Cl bond lengths and Co...Co distances (Table 2) revealed the following tendency. The Co—Cl distances in the mononuclear and Co(μ-Cl)₂Co complexes is noticeably (by ~0.1 Å) shorter than those found for compounds **1**. In other words, transition from the isolated Co—Cl fragment to the polymeric network, where each two Co atoms are linked by one

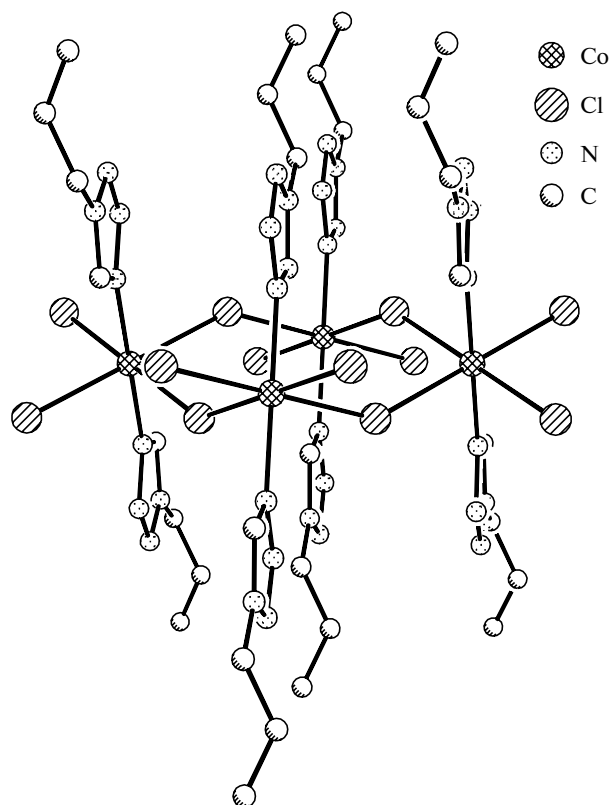


Fig. 2. Structure of the polymeric layer of complex **1**. The H atoms and second positions of the allyl substituent are not shown.

chloride bridge, elongates the Co—Cl bonds. At the same time, transition to the chain, where pairs of the Co atoms are linked by two Cl atoms, does not virtually change the length of these bonds. Finally, the Co—Cl bonds are

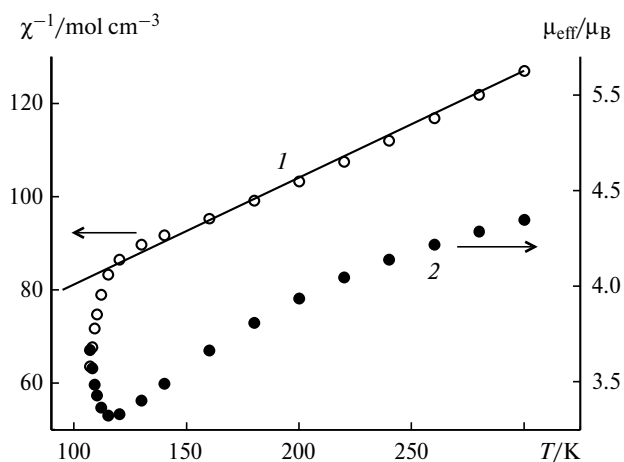


Fig. 3. Temperature plots of χ^{-1} (1) and μ_{eff} (2) for complex **1** at temperatures higher than the ordering temperature. The solid line corresponds to the Curie—Weiss equation.

slightly elongated in the complexes with three bridging Cl atoms. The Co...Co distances are long in all these compounds, indicating the absence of direct metal—metal interactions. An increase in the number of the bridging Cl atoms in these complexes regularly shortens this distance.

At 300 K, μ_{eff} for complex **1** is $4.3 \mu_{\text{B}}$, which is higher than the purely spin value ($3.87 \mu_{\text{B}}$) due to the significant orbital contribution to the magnetic moment from the cobalt(II) ions. The temperature decrease results in a decrease in μ_{eff} , which gives evidence that antiferromagnetic exchange interactions between unpaired electrons of the metal ions predominate (Fig. 3). This is the difference of compound **1** from the copper(II) complexes with the similar structure, where ferromagnetic interactions predominate.³ In the 130–300 K temperature interval, the

Table 2. The Co—Cl and Co—Co bond lengths (d) and ordering temperatures (T_{N}) of some cobalt(II) chloride complexes

Compound	$d(\text{Co—Cl})$	$d(\text{Co—Co})$	T_{N}/K	Refs.
	\AA			
Mononuclear complexes				
<i>cis</i> -[CoCl ₂ (H ₂ O) ₄]	2.408, 2.421	—	—	7
<i>trans</i> -[CoCl ₂ (H ₂ O) ₄] · 2H ₂ O	2×2.424	—	2.29	8
<i>trans</i> -[Co{C(NH ₂) ₂ NHNH ₂ } ₂ Cl ₄]	2×2.454, 2×2.465	—	—	9
Molecular complexes Co(μ-Cl) ₂ Co				
[Co ₂ Cl ₂ (C ₄ O ₂ H ₁₀) ₂](SbCl ₆) ₂	2.364, 2.388	3.432	—	10
[Co ₂ Cl ₂ (C ₁₁ H ₁₃ NO ₄) ₂]	2.310, 2.553	3.557	—	11
[Co ₂ Cl ₂ (2-C ₈ H ₁₂ NO ₂) ₂]	2×2.416, 2×2.438	3.574	—	12
Chain complexes Co(μ-Cl) ₂ Co				
<i>trans</i> -[Co(H ₂ O) ₂ Cl _{4/2}] _∞	2×2.460, 2×2.471	3.564	17.2	13, 14
[(Me ₃ NH)[Co(H ₂ O) ₂ Cl _{4/2}]Cl] _∞	2×2.456, 2×2.503	3.636	4.13	14, 15
[CoPy ₂ Cl _{4/2}] _∞	4×2.49	3.593	3.17	14, 15
Complex Co(μ-Cl) ₃ Co				
[Co ₂ Cl ₃ (C ₉ H ₂₁ N ₃) ₂] · BPh ₄	2.444—2.525	3.048, 3.062	—	16

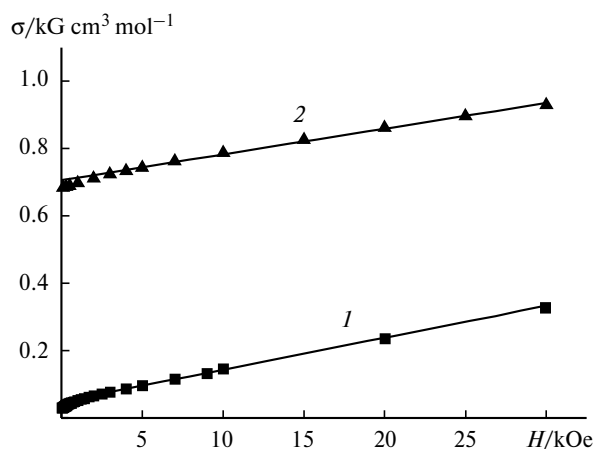


Fig. 4. Main magnetization curves for complex **1** measured after cooling in the magnetic fields with the intensity $H_{\text{cool}} = 5$ (1) and 100 Oe (2).

Curie–Weiss law $\chi = C/(T - \theta)$ is obeyed with the parameters $C = 4.36 \pm 0.09 \text{ cm}^3 \text{ K mol}^{-1}$, $\theta = -240 \pm 10 \text{ K}$. Upon further cooling to $102 \pm 1 \text{ K}$, complex **1** is transformed into the magnetically ordered state. Below this temperature, the magnetic characteristics of the sample depend, to a great extent, on the intensity of the magnetic field in which the sample was cooled (H_{cool}). The magnetization curves $\sigma(H)$ measured after cooling in a low field of $\sim 5 \pm 2 \text{ Oe}$ and in a field of 100 Oe are presented in Fig. 4. In both cases, the $\sigma(H)$ plots obey the equation $\sigma(H) = \sigma_S + \chi H$, where σ_S is the spontaneous magnetization. The σ_S values differ substantially, being 48 ± 1 and $710 \pm 5 \text{ G cm}^3 \text{ mol}^{-1}$ for H_{cool} equal to 5 and 100 Oe, respectively. An increase in H_{cool} higher than 100 Oe does not further increase σ_S , and the maximum spontaneous magnetic moment is $710 \text{ G cm}^3 \text{ mol}^{-1}$. Magnetization reversal of complex **1** results in hysteresis (Fig. 5). The hysteresis loop is displaced along the ordinate. The displacement value is determined by the intensity of the

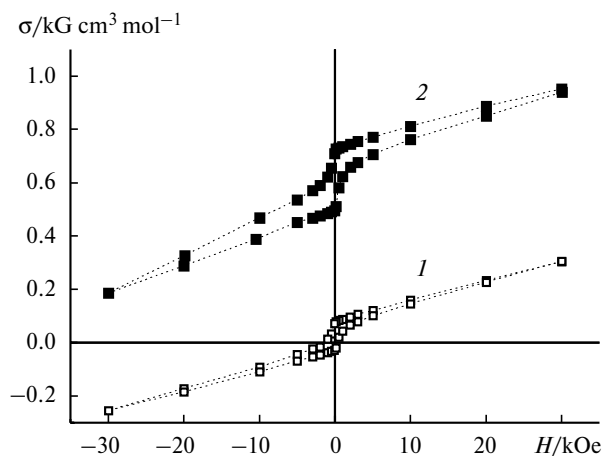


Fig. 5. Change in the hysteresis loop for different intensities of the initial cooling field: $H_{\text{cool}} = 5$ (1) and $3 \cdot 10^4 \text{ Oe}$ (2), $T = 5 \text{ K}$.

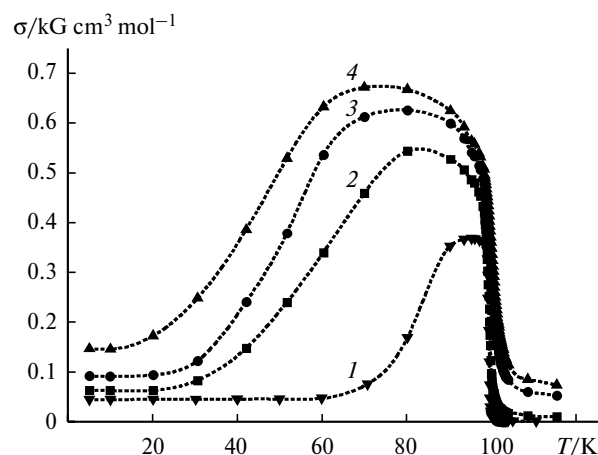


Fig. 6. Temperature plots of the magnetization (σ) for sample **1** measured in magnetic fields with different intensities: $H_{\text{meas}} = 0.1$ (1), 1 (2), 5 (3), and 7 kOe (4); $H_{\text{cool}} = 5 \text{ Oe}$.

magnetic field in which the sample was cooled. The width of the hysteresis loop is independent of H_{cool} within the experimental error, being $600 \pm 20 \text{ Oe}$ at 5 K. The temperature plot of the magnetization for measurements in fields with different intensities after cooling of the sample in the zero magnetic field is shown in Fig. 6. The magnetization $\sigma(T)$ increases in these curves at different temperatures depending on the applied magnetic field, while the sharp decrease in $\sigma(T)$ in the transition point is independent of the field of measurement. The $\sigma(T)$ curves obtained during cooling or measured on heating of the sample after cooling in the fields $> 100 \text{ Oe}$ are identical.

Despite the specificity of the magnetic behavior of the complex under study at different intensities of the initial cooling field, we believe that compound **1** is an antiferromagnetic with weak ferromagnetism with $T_N = 102 \pm 1 \text{ K}$ and $\sigma_S(5 \text{ K}) = 710 \pm 5 \text{ G cm}^3 \text{ mol}^{-1}$. The spontaneous moment can originate from the noncollinearity of the magnetic sublattices of the Co^{II} ions in complex **1**. The estimate of the slope angle of the magnetic sublattices is $\sim 2.5^\circ$ for the theoretical saturation magnetization of $16755 \text{ G cm}^3 \text{ mol}^{-1}$ of the ordered spins $S = 3/2$ with the g factor equal to 2.

The observed $\sigma(T, H)$ plots and hysteresis phenomena in the crystal of **1** are likely related to the polycrystallinity of the sample and the strong magnetic anisotropy, which is characteristic of the Co^{II} ions. For example, when the field is applied along the Z axis, the expression for the energy takes the form $\mu H + k\mu_Z$, where k is the anisotropy constant. At $H_{\text{cool}} \rightarrow 0$, in each crystallite of the sample the vector of spontaneous magnetization is directed along the axis of light magnetization and, correspondingly, the mean moment of the whole sample is equal to zero. In this case, the magnetization reversal occurs along the symmetrical loop. Cooling in the magnetic field results in the preferential orientation of the magnetic moments along

the field. Since $k < 0$, the magnetization reversal of the sample occurs along the displaced hysteresis loop under the conditions where $k\mu_Z > \mu H$. It can be assumed that in complex **1** the module of the anisotropy constant is so high that the condition $k\mu_Z > \mu H$ is fulfilled in the whole interval of the experimentally studied magnetic fields. The behavior of the unusual $\sigma(T, H)$ plots (see Fig. 6) can be due to the fact that the anisotropy constant decreases more rapidly with temperature than the spontaneous magnetization. For this reason, the contributions from $k\mu_Z$ and μH become equal with an increase in the external magnetic field intensity and, correspondingly, the spontaneous magnetization increases.

According to the published magnetochemical data, several cobalt(II) chloride complexes undergo phase transition to the magnetically ordered state. For all these compounds, the ground state is antiferromagnetic below the ordering temperature; their T_N values are presented in Table 2. Weak ferromagnetism has previously^{14,15} been found for the *trans*-[Co(H₂O)₂Cl_{4/2}]_∞ and [(Me₃NH)[Co(H₂O)₂Cl_{4/2}]Cl]_∞ complexes, although the spontaneous magnetization values were not presented. It is difficult to reveal the nature of the weak ferromagnetic moment¹⁵ because both the monoionic anisotropy,¹⁷ antisymmetrical hyperexchange,¹⁷ and anisotropy of the g factor¹⁸ can be a reason for the slope of the magnetic sublattices. As can be seen from the data in Table 2, the transition temperature in compound **1** is an order of magnitude higher than that in the previously studied cobalt(II) chloride complexes. Perhaps, this is due to the layered-polymeric structure of crystal **1**.

Based on the structure and specificity of its behavior, complex **1** can be ascribed to a wide class of compounds named molecular magnets.¹⁹ As a new molecular magnet, complex **1** combines the properties corresponding to the purposes of molecular design: the kinetic stability under normal conditions, a high (for molecular magnets) temperature of magnetic ordering, and a possibility of further functionalization of the complex.

This work was financially supported by the Russian Foundation for Basic Research (Project Nos. 02-03-06184 and 02-07-90322).

References

1. L. G. Lavrenova, A. N. Bogatkov, L. A. Sheludyakova, V. N. Ikorskii, S. V. Larionov, and P. N. Gaponik, *Zh. Neorg. Khim.*, 1991, **36**, 1220 [*J. Inorg. Chem. USSR*, 1991, **36**, 693 (Engl. Transl.)].
2. L. G. Lavrenova, V. N. Ikorskii, and S. V. Larionov, *Zh. Neorg. Khim.*, 1993, **38**, 1517 [*J. Inorg. Chem. USSR*, 1993, **38**, 1416 (Engl. Transl.)].
3. L. G. Lavrenova, A. N. Bogatkov, V. N. Ikorskii, L. A. Sheludyakova, E. G. Boguslavskii, P. N. Gaponik, and S. V. Larionov, *Zh. Neorg. Khim.*, 1996, **41**, 423 [*Russ. J. Inorg. Chem.*, 1996, **41**, 406 (Engl. Transl.)].
4. A. V. Virovets, I. A. Baidina, V. I. Alekseev, N. V. Podberezskaya, and L. G. Lavrenova, *Zh. Strukt. Khim.*, 1996, **37**, 330 [*Russ. J. Struct. Chem.*, 1996, **37**, 288 (Engl. Transl.)].
5. A. V. Virovets, N. V. Podberezskaya, L. G. Lavrenova, and G. A. Bikzhanova, *Acta Crystallogr., Sect. C.*, 1995, **51**, 1084.
6. F. H. Allen and O. Kennard, *Chemical Design Automatic News*, 1993, **8**, 31.
7. K. Waizumi, H. Masuda, H. Ohtaki, K. Tsukamoto, and I. Sunagawa, *Bull. Chem. Soc. Jpn.*, 1990, **63**, 3426.
8. Z. M. El Saffar, *J. Phys. Soc. Jpn.*, 1962, **17**, 1334.
9. A. E. Shvelashvili, E. V. Miminoshvili, V. K. Bel'skii, and T. O. Vardosanidze, *Zh. Neorg. Khim.*, 1998, **43**, 255 [*Russ. J. Inorg. Chem.*, 1998, **43**, 201 (Engl. Transl.)].
10. A. J. Kinneging, W. J. Vermin, and S. Gorter, *Acta Crystallogr., Sect. B.*, 1982, **38**, 1824.
11. G. Singh and D. B. Sowerby, *J. Chem. Soc., Dalton Trans.*, 1977, 490.
12. C. Hemmert, M. Renz, H. Gornitzka, S. Soulet, and B. Meunier, *Chem. Europ. J.*, 1999, **5**, 1766.
13. B. Morosin, *J. Chem. Phys.*, 1966, **44**, 252.
14. R. Navarro and L. J. de Jongh, *Physica, B*, 1978, **94**, 67.
15. D. B. Losee, J. N. McElearney, G. E. Shankle, and R. L. Carlin, *Phys. Rev., B*, 1973, **8**, 2185.
16. U. Bossek, D. Nuhlen, E. Bill, T. Glaser, C. Krebs, T. Weyhermuller, K. Wieghardt, M. Lengen, and A. Trautwein, *Inorg. Chem.*, 1997, **36**, 2834.
17. T. Moriya, *Phys. Rev.*, 1960, **120**, 90.
18. I. F. Silvera, J. H. M. Thornley, and M. Tinkham, *Phys. Rev.*, 1964, **136**, A695.
19. V. I. Ovcharenko and R. Z. Sagdeev, *Usp. Khim.*, 1999, **68**, 381 [*Russ. Chem. Rev.*, 1999, **68**, 345 (Engl. Transl.)].

Received September 25, 2002;
in revised form January 13, 2003